Figure S1

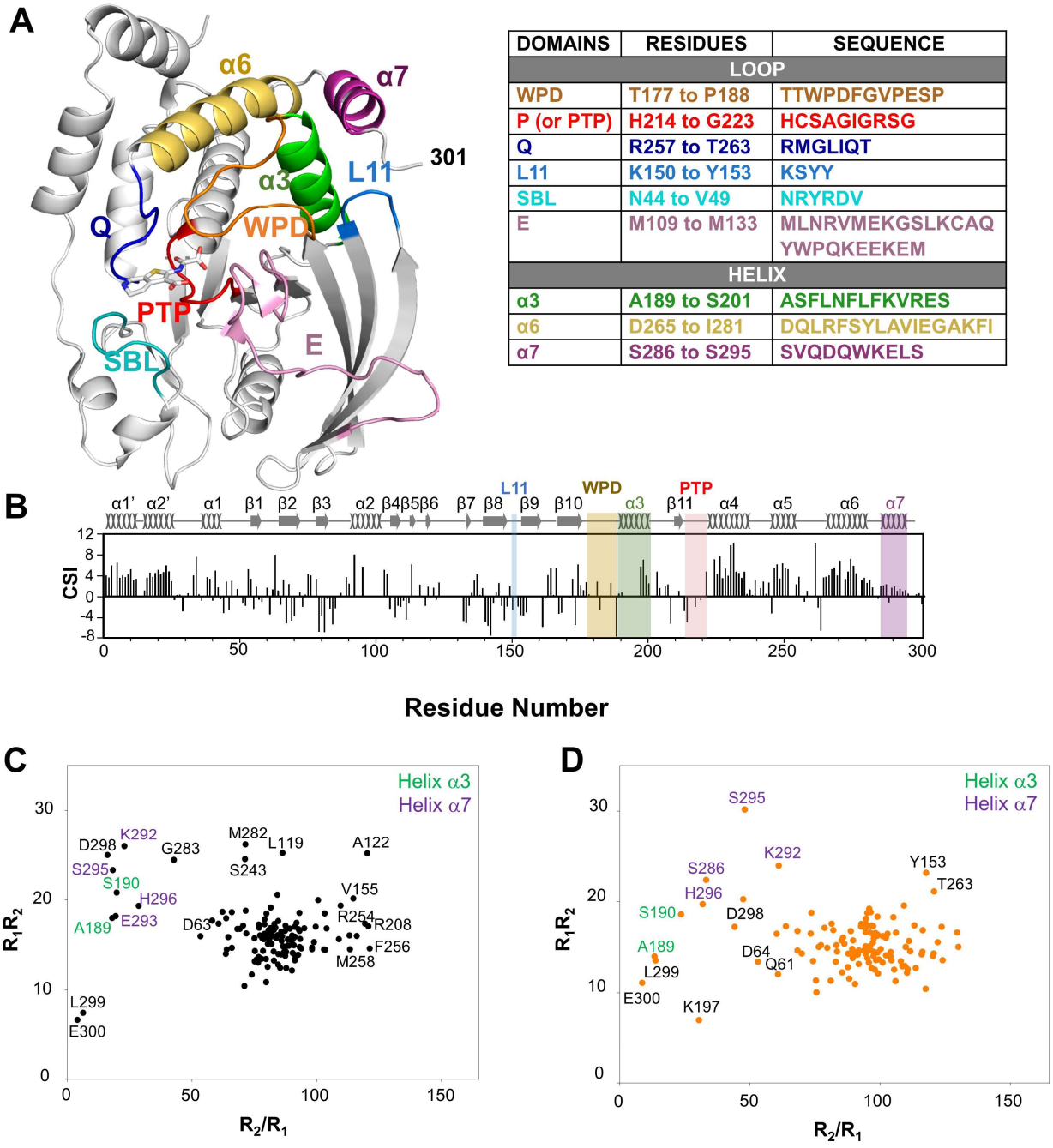

DOMAINS	RESIDUES	SEQUENCE
LOOP		
WPD	T177 to P188	TTWPDFGVPESP
P (or PTP)	H214 to G223	HCSAGIGRSG
Q	R257 to T263	RMGLIQT
L11	K150 to Y153	KSYY
SBL	N44 to V49	NRYRDV
E	M109 to M133	MLNRVMEKGSLKCAQ YWPQKEEKEM
HELIX		
α3	A189 to S201	ASFLNFLFKVRES
α6	D265 to I281	DQLRFSYLAVIEGAKFI
α7	S286 to S295	SVQDQWKELS

Figure S1. PTP1B*, related to Figure 1.*

(A) Domains of PTP1B, with key PTP1B structural elements color coded and described as indicated. The TCS401 inhibitor is shown in sticks (PDB: 5K9W).

(B) Chemical shift index (CSI) analysis of $PTP1B_{1\text{-}301}$ (the catalytic domain). The protein secondary structures are identified using program CSI 2.0 based on backbone chemical shift of $^{13}C_{\alpha}$ and $^{13}C_{\beta}$ and PTP1B sequence. L11 (blue), WPD (brown), α3 (green), PTP (red) and α7 (purple) residues are highlighted.

(C) Bracken plot of backbone ^{15}N relaxation data for PTP1B.

(D) Bracken plot of backbone ^{15}N relaxation data for PTP1B:TCS401.

Figure S2

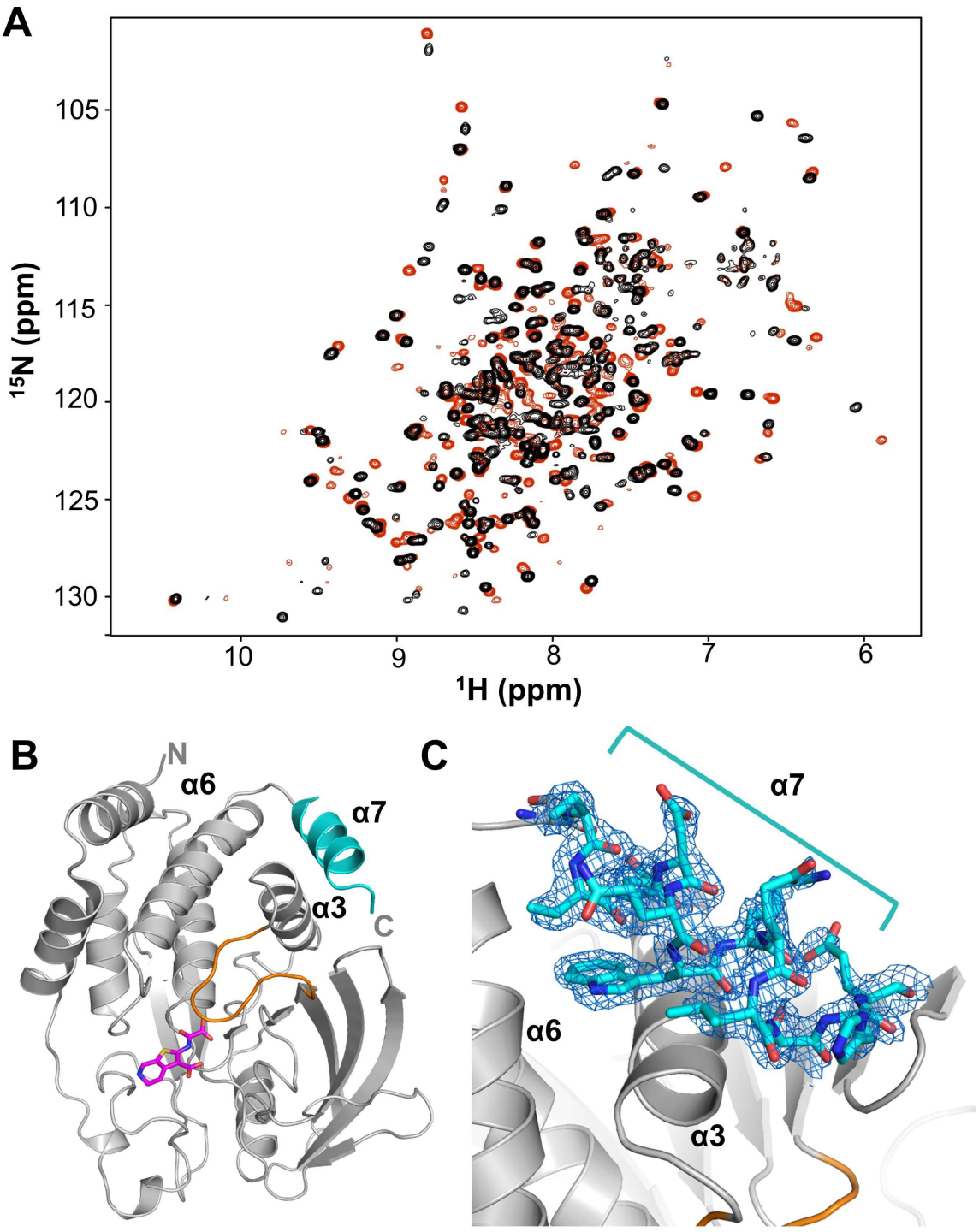

Figure S2. PTP1B helix α7 becomes ordered upon binding TCS401, *related to Figure 1*.
(A) Overlay of the 2D [^{1}H-^{15}N] TROSY spectra of PTP1B (black) and PTP1B:TCS401 (1:3 molar ratio, red). Spectra were recorded at 298 K at a proton resonance frequency of 850 MHz.
(B) Crystal structure of the PTP1B:TCS401 complex (PDB: 5K9W). TCS401 is shown as sticks (pink), the closed PTP loop in orange and the ordered C-terminal helix α7 (cyan).
(C) Electron density map (2Fo-Fc, σ=1.0) of PTP1B helix α7 (cyan; residues 286-295, bracket).

Figure S3

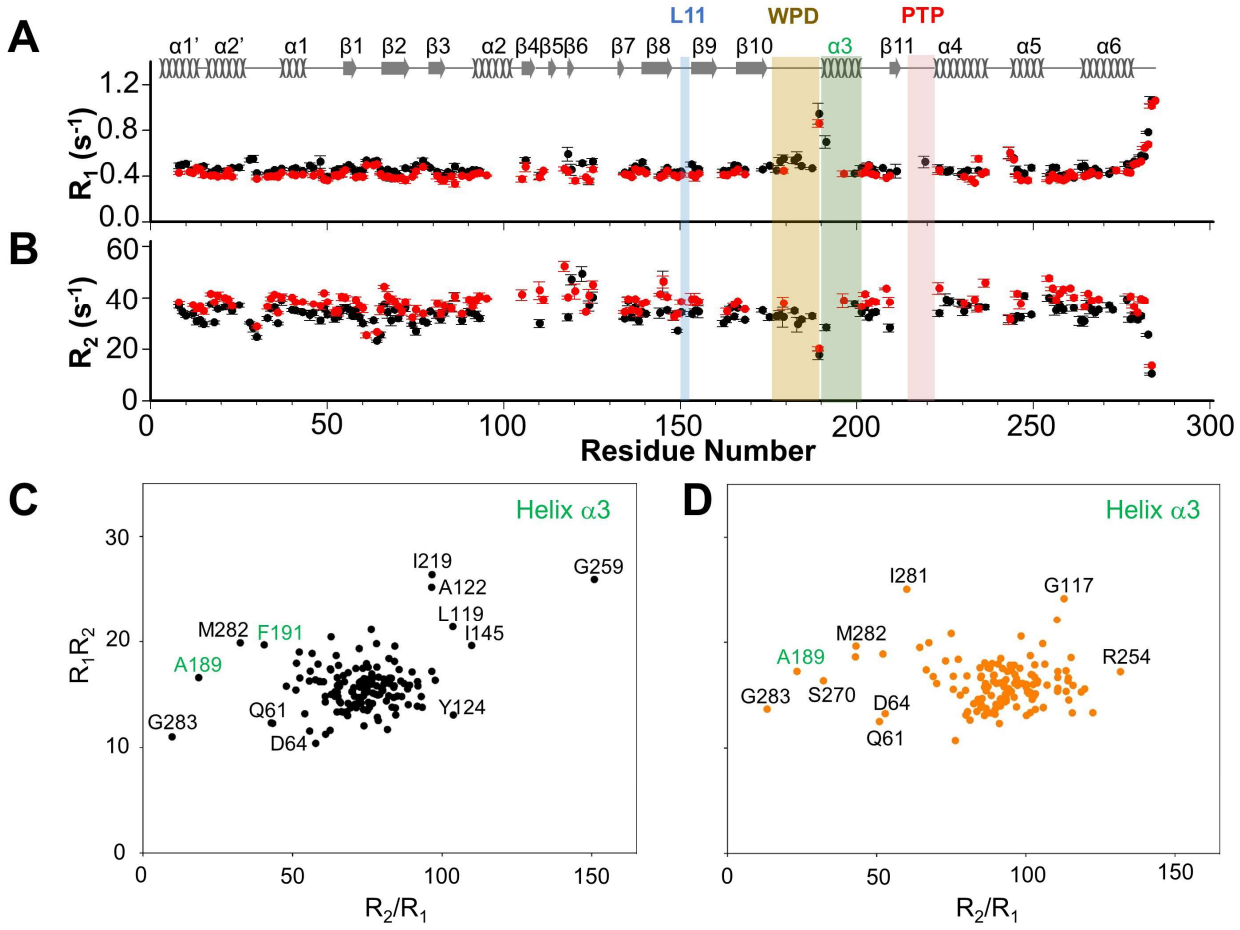

Figure S3. **Relaxation data for PTP1BΔ7 (residues 1-284); *related to Figure 2*.**
(A) ^{15}N longitudinal R_1 relaxation rates for PTP1BΔ7 (black) and PTP1BΔ7:TCS401 (red).
(B) Transverse R_2 relaxation rates for PTP1BΔ7 (black) and PTP1BΔ7:TCS401 (red). L11 (blue), WPD (brown), α3 (green) and PTP (red) residues are highlighted.
(C) Bracken plot of backbone ^{15}N relaxation data for PTP1BΔ7.
(D) Bracken plot of backbone ^{15}N relaxation data for PTP1BΔ7:TCS401.

Figure S4

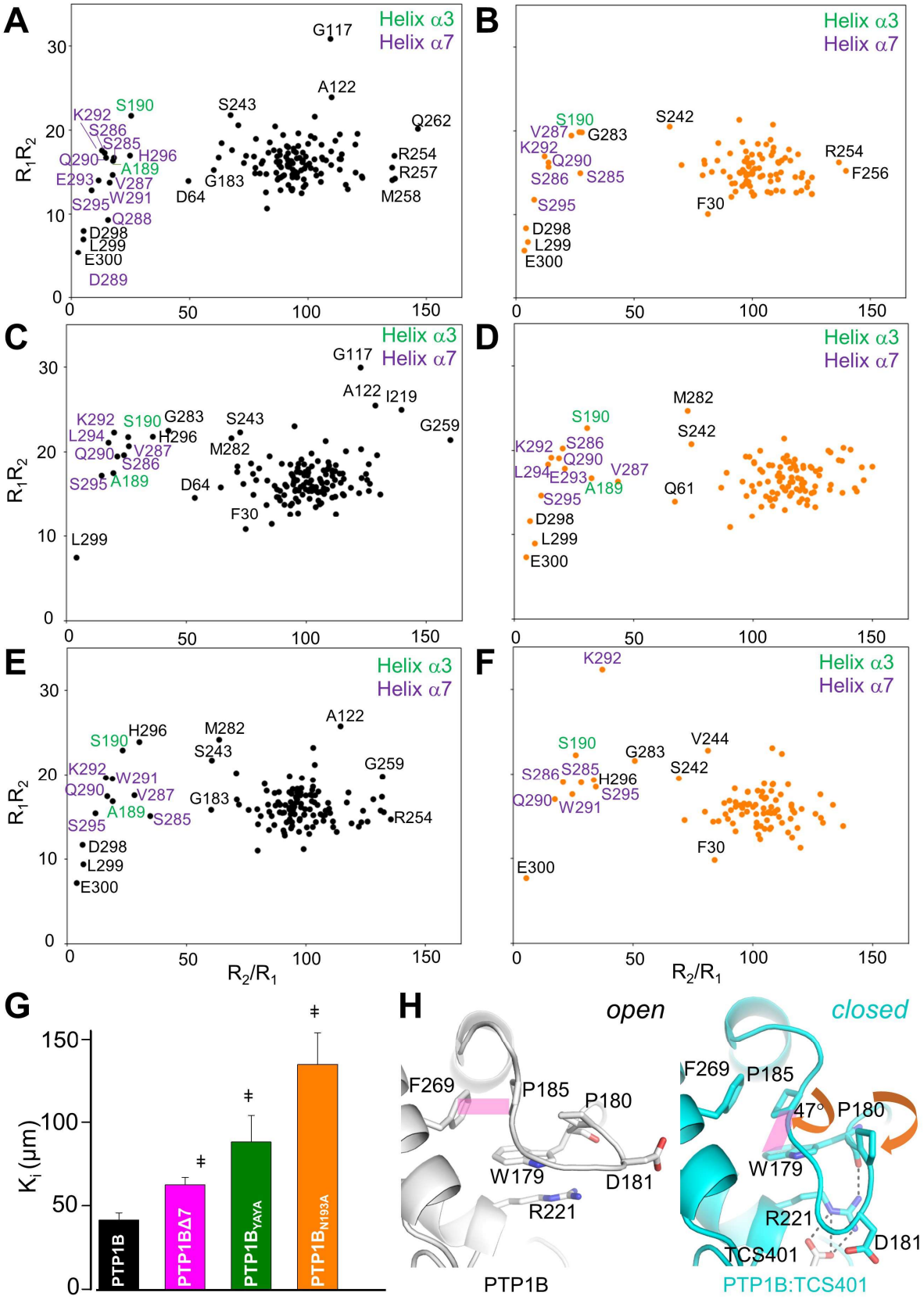
A
B
C
D
E
F
G
H
Helix α3
Helix α7
R1R2
R2/R1
Ki (μm)
PTP1B
PTP1BΔ7
PTP1BYAYA
PTP1BN193A
open
closed
PTP1B
PTP1B:TCS401
47°
W179
R221
D181
F269
P185
P180
TCS401

Figure S4. Relaxation and activity data for PTP1B allosteric variants, *related to Figure 3*.
(A) Bracken plot of backbone ^{15}N relaxation data for $PTP1B_{YAYA}$.
(B) Bracken plot of backbone ^{15}N relaxation data for $PTP1B_{YAYA}$:TCS401.
(C) Bracken plot of backbone ^{15}N relaxation data for $PTP1B_{N193A}$.
(D) Bracken plot of backbone ^{15}N relaxation data for $PTP1B_{N193A}$:TCS401.
(E) Bracken plot of backbone ^{15}N relaxation data for $PTP1B_{T178A}$.
(F) Bracken plot of backbone ^{15}N relaxation data for $PTP1B_{T178A}$:TCS401.
(G) K_i values of PTP1B and mutants by TCS401 (±SE, n=3-9, ǂt-test, $p < 0.05$).
(**H)** Role of P185 in WPD loop closure. P180 is perpendicular to P185 in PTP1B open state (gray, PDB: 5K9V). In the closed state (cyan, PDB: 5K9W), P180 rotates ~90° due to the formation of hydrogen bond between backbone of W179 and side chain of R211, facilitating the closure of WPD loop. CH/π stacking between P185, F269 and W179 is shaded in pink.

Figure S5

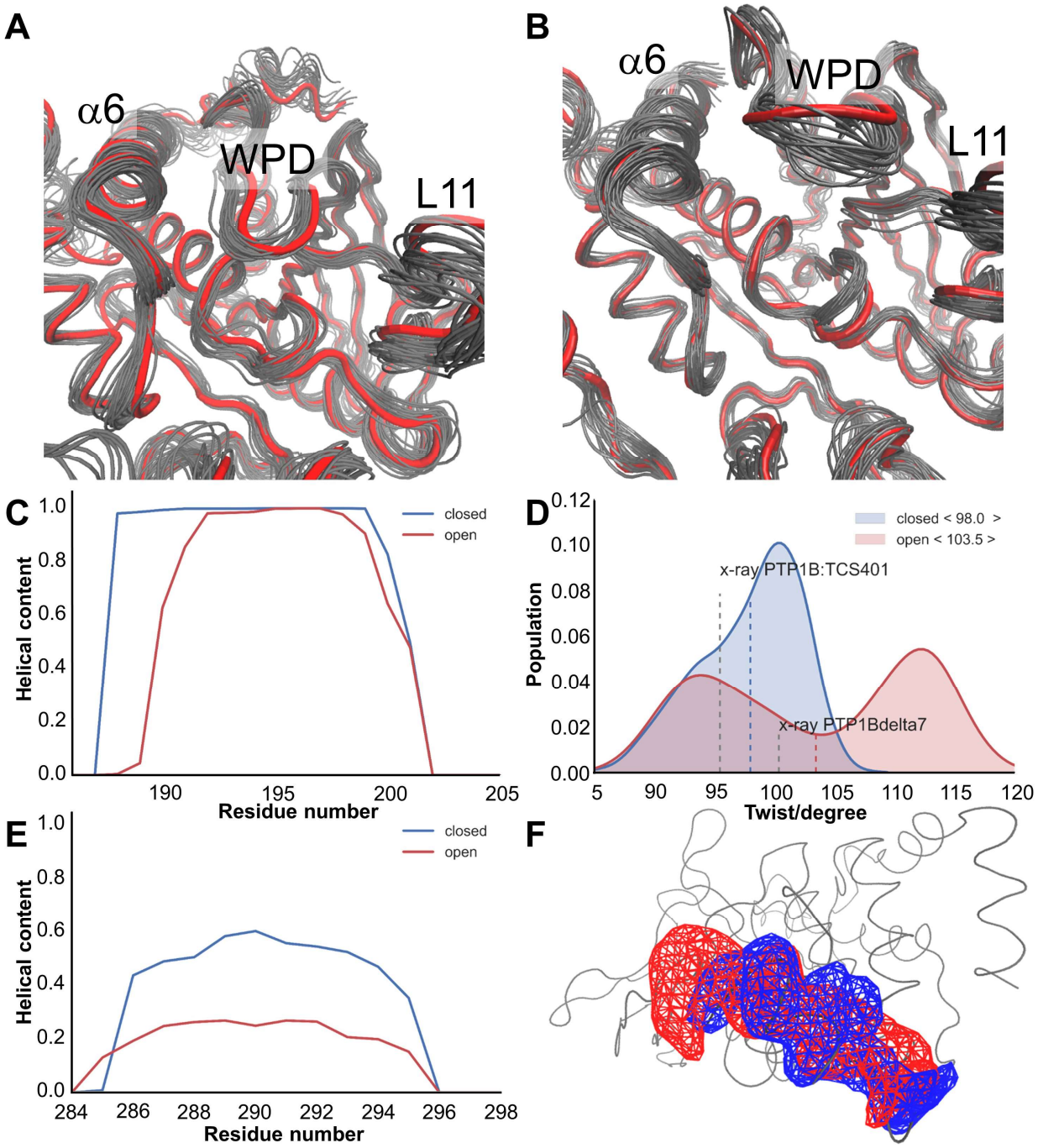

Figure S5. PTP1B chemical shift restrained molecular dynamics, *related to Figure 5.*
(A) Superposition of 32 structures from the unbiased MD (gray tubes) using PTP1B:TCS401 (PDB: 5K9W) as starting structure (red tube). The WPD stays closed.
(B) Superposition of 32 structures from the unbiased MD (gray tubes) using PTP1BΔ7 (PDB: 5KA0) as starting structure (red tube).

(C) Helix α3 shortens/twists when the WPD loop opens. Helical content of α3 in the open (red) and closed (blue) state, showing that 2 residues on the N-terminus of the helix unfold (melt) in the open state of the WPD loop.
(D) Unit-twist of an N-terminal turn of α3 (residues 190-193) showing the twisting of the N-terminus of α3.
(E) Helix α7 appears less well-ordered in the open state. Helical content of α7 in the open (red) and closed (blue) state, showing that α7 melts in the open state of the WPD loop.
(F) Overall structure of α7 represented by the occupancy averaged over open (red) and closed (blue) trajectory frames. It can be seen that in the closed form the overall helical shape is contained on average, whereas in the open state α7 is more extended and less ordered.

Table S1. Inhibitor $K_{D,}$ turnover rates (k_{cat}) and catalytic efficiencies (k_{cat}/K_m) of PTP1B and its variants; *related to Figure 1.*

PTP1B variant	**TCS401 K_D (μM)**	**Allosteric Inhibitor K_D (μM)**	**k_{cat} (s^{-1})**	**k_{cat}/K_m ($x10^3$ $M^{-1}s^{-1}$)**
PTP1B	26 ± 1.8	7.8 ± 0.8	4.4 ± 0.4	5.0 ± 0.8
PTP1BΔ7	33 ± 5.6	21 ± 1.6*	2.8 ± 0.3	2.1 ± 0.1*
$PTP1B_{L192A}$	39 ± 6	22 ± 0.8*	0.5 ± 0.03*	0.46 ± 0.04*
$PTP1B_{N193A}$	37 ± 4	13 ± 0.6*#	2.5 ± 0.2*	1.8 ± 0.3*
$PTP1B_{YAYA}$	26 ± 3	12 ± 0.7*#	3.1 ± 0.1*	2.3 ± 0.1*
$PTP1B_{Y152F}$	n.d.	n.d.	3.2 ± 0.09*	3.4 ± 0.06*
$PTP1B_{Y153F}$	n.d.	n.d.	3.3 ± 0.03*	3.7 ± 0.5*
$PTP1B_{Y152A}$	n.d.	n.d.	2.9 ± 0.1*	3.1 ± 0.08*
$PTP1B_{Y153A}$	n.d.	n.d.	3.6 ± 0.04*	3.9 ± 0.4*
$PTP1B_{T178A}$	45 ± 3.5*	n.d.	2.5 ± 0.03*	1.7 ± 0.1*
$PTP1B_{P185G}$	20 ± 0.6*	n.d.	0.08 ± 0.002*	0.1 ± 0.03*
$PTP1BΔ7_{P185G}$	21 ± 3.6	n.d.	0.09 ± 0.002*#	0.1 ± 0.05*#
$PTP1B_{V184G}$	31 ± 1.8	n.d.	0.4 ± 0.02*	0.5 ± 0.05*
$PTP1BΔ7_{V184G}$	35 ± 2.7	n.d.	0.6 ± 0.02*#	0.4 ± 0.02*#
$PTP1B_{Y176G}$	34 ± 4	n.d.	1.4 ± 0.04*	1.4 ± 0.07*
$PTP1B_{T177G}$	34 ± 5.4	n.d.	6.0 ± 0.002	23.0 ± 0.7*
$PTP1BΔ7_{T177G}$	n.d	n.d.	6.0 ± 0.002#	19 ± 0.8*#

*statistically significant difference between PTP1B and variants, t-test, $p<0.05$
#statistically significant difference between PTP1BΔ7 and variants, t-test, $p<0.05$
n.d. not determined

Table S2. Melting temperatures (T_M) of PTP1B and variants, *related to Figure 1*.

PTP1B variant	**T_M (°C)**
PTP1B	54.7
PTP1BΔ7	53.5
$PTP1B_{L192A}$	51.3
$PTP1B_{N193A}$	49.0
$PTP1B_{YAYA}$	50.4
$PTP1B_{T178A}$	60.0
$PTP1B_{P185G}$	47.3
$PTP1BΔ7_{P185G}$	45.3
$PTP1B_{V184G}$	47.4
$PTP1BΔ7_{V184G}$	45.7
$PTP1B_{Y176G}$	40.7
$PTP1BΔ7_{T177G}$	47.3

Table S3. Catalytic efficiency and inhibition constants of PTP1B and variant activity by TCS-401, *related to Figure 1.*

PTP1B variant	**k_{cat}/K_m (x 10^3 $M^{-1}s^{-1}$)**	**k_{cat}/K_m (x 10^3 $M^{-1}s^{-1}$) TCS401 100 µM**	**k_{cat}/K_m (x 10^3 $M^{-1}s^{-1}$) TCS401 300 µM**	**K_i (µM)**
PTP1B	5.0 ± 0.8	1.1 ± 0.08‡	0.5 ± 0.04‡	41 ± 4.4
PTP1BΔ7	2.1 ± 0.1*	0.7 ± 0.07*	0.3 ± 0.03*	63 ± 4.4*
$PTP1B_{N193A}$	1.8 ± 0.3*	0.9 ± 0.08‡	0.5 ± 0.04‡	135 ± 19*
$PTP1B_{YAYA}$	2.3 ± 0.1*	1.0 ± 0.07*	0.6 ± 0.02‡	88 ± 16*

*statistically significant difference between PTP1B and variants, t-test, $p<0.05$
‡statistically significant difference between Cr and TCS, paired t-test, $p<0.05$

Table S4. Key allosteric residues in PTP1B, *related to Figure 6*.

Key allosteric residues in PTP1B	Number of PTPs with allosteric residue conserved	% conservation in PTP family*	Identity of the residues present in PTPs for which the allosteric residue is not conserved°	Conservation in PTP1B & TCPTP (%)
Y152	4	11	D(12), E(8), T(4), C(3), A(2), N(2), G(1), H(1)	100
Y153	25	68	F(5), W(5), H(1), I(1)	100
T178	4	11	S(12), A(11), D(2), G(2), N(2), Q(2), K(1), V(1)	100
P185	37	100		100
S187	13	35	D(6), Y(5), H(4), T(4), A(1), E(1), N(1), Q(1), R(1)	100
S190	8	22	P(11), G(10), D(3), L(2), H(1), I(1), N(1)	100
F191	9	24	L(15), I(4), V(4), M (3), A(1), N(1)	100
L192	31	84	I(4), F(2)	100
N193	2	5	D(6), A(5), K(4), S(4), R(3), Q(3), T(3), E(2), G(2), H(2), W(1)	100
F269	33	89	L(3), Y(1)	100

*Total number of the classic PTPs of human=37.
°Numbers in parentheses indicate the number of PTPs with that residue.